Ferritin–EGFP Chimera as an Endogenous Dual-Reporter for Both Fluorescence and Magnetic Resonance Imaging in Human Glioma U251 Cells

Caihong Jiang[1], Dongmei Wu[1], and E. Mark Haacke[1,2]

[1]Shanghai Key Laboratory of Magnetic Resonance, East China Normal University, Shanghai, China and [2]Department of Radiology, Wayne State University, Detroit, Michigan

Corresponding Author:
E. Mark Haacke, PhD
WSU MR Research Facility,
HUH-MR Research/Radiology,
3990 John R Street,
Detroit, Michigan 48201;
E-mail: nmrimaging@aol.com

Key Words: ferritin, EGFP, dual-reporter human glioma U251 cells, tetracycline-regulated system, MRI

Abbreviations: Enhanced green fluorescent protein (EGFP), magnetic resonance imaging (MRI), Dulbecco's modified Eagle's medium (DMEM), fetal bovine serum (FBS), phosphate-buffered saline (PBS), 3-(4,5-dimethyl-2-thiazolyl)-2,5-diphenyl-2-H-tetrazolium bromide dimethyl sulfoxide (MTT), ferric citrate ammonium (FAC), inductively coupled plasma mass spectroscopy (ICP-MS), tetracycline repressor protein (TetR), tetracycline (Tet)

ABSTRACT

A unique hybrid protein ferritin–enhanced green fluorescent protein (EGFP) was built to serve as an endogenous dual reporter for both fluorescence and magnetic resonance imaging (MRI). It consists of a human ferritin heavy chain (an iron-storage protein) at the N terminus, a flexible polypeptide in the middle as a linker, and an EGFP at the C terminus. Through antibiotic screening, we established stable human glioma U251 cell strains that expressed ferritin–EGFP under the control of tetracycline. These cells emitted bright green fluorescence and were easily detected by a fluorescent microscope. Ferritin–EGFP overexpression proved effective in triggering obvious intracellular iron accumulation as shown by Prussian blue staining and by MRI. Further, we found that ferritin–EGFP overexpression did not cause proliferation differences between experimental and control group cells when ferritin–EGFP was expressed for <96 hours. Application of this novel ferritin–EGFP chimera has a promising future for combined optical and MRI approaches to study in vivo imaging at a cellular level.

INTRODUCTION

Glioma is among one of the most malignant tumors and is characterized by high levels of mortality and recurrence (1). Further, glioma cells show infiltrative growth and have no obvious boundaries with surrounding normal tissues. Precise noninvasive imaging is of great importance in tumor localization, metastasis detection, and subsequent therapy. Fluorescence imaging can provide noninvasive real-time dynamic observation of tumors. However, fluorescence has poor penetration capability, limiting its usage in deep-seated tumors. In contrast, magnetic resonance imaging (MRI) is not affected by the depth of target tissues and has high spatial resolution. However, the sensitivity of MRI is not high enough for performing cellular or molecular imaging. Therefore, to solve this problem, MRI contrast agents were invented using substances such as iron or gadolinium (2, 3). For example, iron oxide nanoparticles are often used in labeling cells (4-6). However, with the division of cells, the exogenous reporter is diluted, leading to a loss of signal change over time. Subsequently, several MRI reporter genes have been introduced into cells by either plasmids or slow virus transfection to serve as endogenous reporters (7, 8).

Our focus will be on the use of ferritin as part of a reporter gene. Ferritin is an extensively studied iron-storage protein in the human body and plays an important role in maintaining the balance of iron metabolism (9, 10). Ferritin is composed of 2 types of subunits, both H and L subunits, namely, the heavy and the light chains. H subunits are the core subunits of iron storage in ferritin and can work as preferable endogenous MRI reporters (11, 12). In recent years, dual reporters that combine the advantages of fluorescence imaging and MRI have gradually become hotspots for noninvasive imaging studies. A dual reporter is usually composed of a fluorescent protein that is used for fluorescence imaging and a ferritin protein that is used for MRI (13-16). However, transgenic ferritin has usually been expressed separately from fluorescent protein and thus is not directly observed by fluorescence detection. There is also some controversy about the effects of ferritin overexpression on cells and in the body (11, 17-20). The reason behind these contradictory facts may be the various ferritin expression levels and different cell types that have been applied in those studies.

Here, we propose an improved dual-reporter ferritin–enhanced green fluorescent protein (EGFP) chimera, with a human

ISSN 2379-1381 http://dx.doi.org/10.18383/j.tom.2015.00181

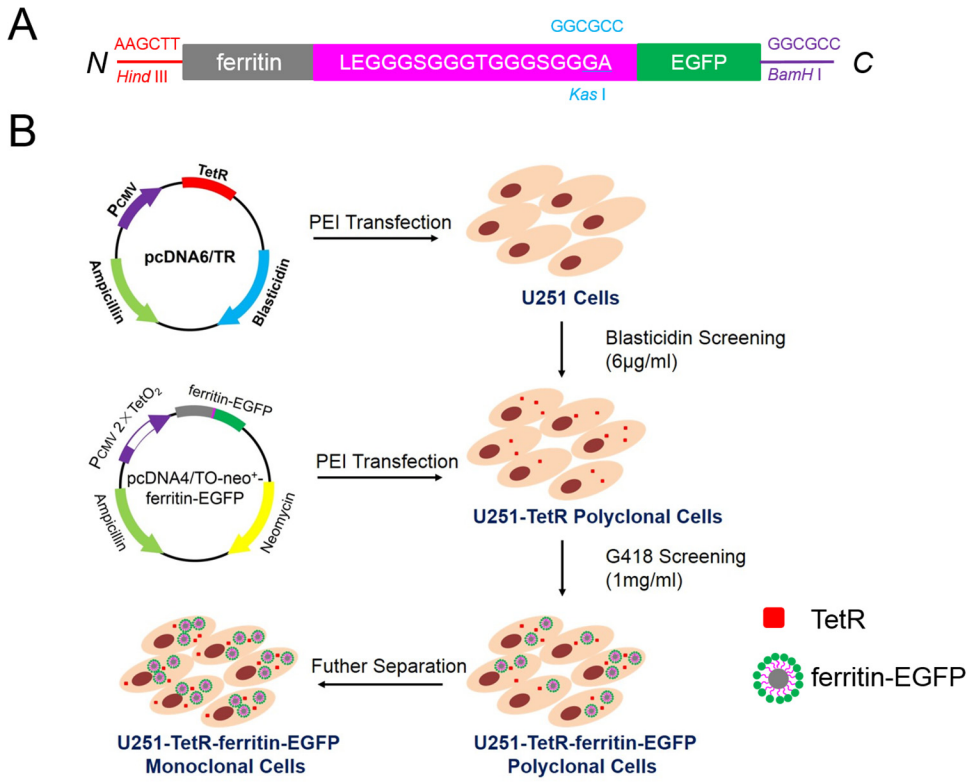

Figure 1. Establishment of tetracycline-inducible U251–tetracycline repressor protein (TetR)–ferritin–EGFP cell strains. The fusion gene of ferritin–EGFP with a human ferritin heavy chain (ferritin) at the N-terminus, a polypeptide (LEGGGSGGGTGGGSGGGA) as a linker in the middle, and an EGFP at the C-terminus (A). Establishment of U251–TetR–ferritin–EGFP mainly through 2 steps of antibiotics' screening (B). First, blasticidin was used to select pcDNA6/TR-transfected U251 cells to get U251–TetR polyclonal cells that expressed TetR at different levels. Second, G418 was further applied to select pcDNA4/TO-neo$^+$–ferritin–EGFP (a modified pcDNA4/TO vector with zeocin replaced by neomycin, and inserted with the ferritin heavy chain–EGFP fusion gene ferritin–EGFP at multiple cloning sites)-transfected U251–TetR polyclonal cells and obtained U251–TetR–ferritin–EGFP polyclonal cells, which were further separated to create U251–TetR–ferritin–EGFP monoclonal cells that expressed tetracycline-inducible ferritin–EGFP at a uniformly high level.

ferritin heavy chain at the N terminus, an EGFP at the C terminus, and a special polypeptide as a linker in the middle that is expected to improve the fluorescence intensity and stability of EGFP (21). By building stable human glioma U251 cell strains that express ferritin–EGFP under the control of tetracycline (Figure 1), we could realize cellular imaging with both fluorescence imaging and MRI techniques.

METHODOLOGY

Gene Constructs

The gene of human ferritin heavy chain (NCBI Reference Sequence: NM_002032.2) with a polypeptide (LEGGGSGGGTGGGSGGGA) at the C-terminus was synthesized with a Hind III restriction site at the 5′-terminus and a Kas I restriction site at the 3′-terminus (Biosune, Shanghai, China). The stop codon of the ferritin gene was deleted. The EGFP gene was generated by polymerase chain reaction amplification using pcDNA3.1-3′-EGFP as templates, with the Kas I restriction site at the 5′-terminus and a BamH I restriction site at the 3′-terminus. pCEP4-ferritin–EGFP was built by insertion of the EGFP gene into pCEP4-ferritin. The above ferritin–EGFP gene was ligated into a modified pcDNA4/TO-neo$^+$ vector (zeocin-resistance gene of pcDNA4/TO was replaced by neomycin-resistance gene) and formed pcDNA4/TO-neo$^+$-ferritin–EGFP. All the above genes were sequenced at Biosune.

Establishment of U251–TetR–Ferritin–EGFP Cell Strains

All transgene constructs were transformed into *Escherichia coli* strain Top10 (Self-made) and transformants with ampicillin resistance. After amplification in *E. coli*, plasmids were extracted by an Axygen mini-preparation kit (Axygen, Hangzhou, China). pCEP4-ferritin–EGFP plasmids were transfected by a self-made polyetherimide-based reagent into HeLa cells to check the ferritin–EGFP expression. Then, pcDNA6/TR vectors (Thermo Fisher Scientific, Shanghai, China) were transfected into human glioma U251 cells (Cell Resource Center of Shanghai Academy of Sciences, Chinese Academy of Sciences, Shanghai, China). Stable U251 cells that expressed tetracycline repressor protein (TetR) were selected using blasticidin (6 μg/mL) (Thermo Fisher Scientific, Shanghai, China) and named U251–TetR cells, which then served as host cells for pcDNA4/TO-neo$^+$-

ferritin–EGFP plasmids transfection. Several U251–TetR–ferritin–EGFP cell strains were generated by G418 screening (1 mg/mL) (Thermo Fisher Scientific, Shanghai, China) and then analyzed by Western blot and fluorescence imaging. Finally, a successful U251–TetR–Ferritin–EGFP cell strain was created that showed stable high-level expression of Ferritin–EGFP under tetracycline regulation. The cell culture medium was Dulbecco's modified Eagle's medium (DMEM) with 10% fetal bovine serum (FBS) (Thermo Fisher Scientific, Shanghai, China).

Western Blot Analysis

Cells were grown on a 6-well cell culture plate (Corning, Shanghai, China) with the same seeding density. Ferritin–EGFP expression was started by adding tetracycline (2 μg/mL) (Aladdin, Shanghai, China) in the culture medium. Then cells were harvested and lysed on ice in a lysis buffer (50 mM Tris HCl, 150 mM NaCl, 1 mM ethylenediaminetetraacetic acid, 10% (v/w) glycerol, 1% (v/w) Triton X-100, and 1 mM phenylmethylsulfonyl fluoride [pH 7.4]) (Aladdin, Shanghai, China). Samples were incubated with a 2× protein loading buffer (Self-made) for 10 minutes at 100°C, and then separated on 10% sodium dodecyl sulfate polyacrylamide gels (self-made) and later transferred to 0.45 μm polyvinylidene fluoride membranes (Millipore, Shanghai, China) for Western blot analysis. Membranes were blocked in the blocking buffer (5% skimmed milk powder in TBST buffer: 0.8% (w/v) NaCl, 0.02% (w/v) KCl, 0.3% Tris base, and 0.05% (v/v) Tween-20, (pH 7.4), for 2 hours at room temperature. Further, membranes were incubated with primary antibodies (CWBIO, Beijing, China) for 1 hour at room temperature, and then with secondary antibodies (CWBIO, Beijing, China) for 1 hour at room temperature. The protein was eventually imaged with Kodak films (Kodak, State of New York, United States) using ECL detection reagent (CWBIO, Beijing, China). Primary antibodies included anti-EGFP polyclonal rabbit antibody (Zen BioScience) and anti-β-actin monoclonal mouse antibody (CWBIO, Beijing, China). Secondary antibodies were horseradish peroxidase-conjugated Goat Anti-Rabbit antibody (CWBIO, Beijing, China) and horseradish peroxidase-conjugated Goat Anti-Mouse antibody (CWBIO, Beijing, China).

Fluorescence Imaging

Cells were cultured in a 6-well cell culture plate in DMEM (10% FBS). Then, DMEM was discarded and cells were washed by phosphate-buffered saline (PBS) (Self-made) 3 times. All fluorescence imaging was performed in the 6-well cell culture plate using a Leica fluorescent microscope (DM4000B, Leica, Solms, Germany). The green fluorescence of EGFP was excited by a blue laser.

Cell Proliferation Assay

Cells were seeded at the same density and cultured in 96-well cell culture plates (Corning, Shanghai, China); 2 groups of cells were tested in this experiment. The first group of cells (U251–TetR–ferritin–EGFP glioma cells) was used to check the effect of ferritin–EGFP expression on cell proliferation. Ferritin–EGFP expression was either started or turned off by adding or withdrawing tetracycline (2 μg/mL) into the cell culture medium. The second group of cells (normal U251 glioma cells) was used to check the effect of tetracycline on cell growth. The experimental group was labeled as tetracycline+ ("Tet+") with 2 μg/mL tetracycline added to the cell culture medium, and the control group was labeled as "Tet−" without any tetracycline in the medium.

Cells were detected every 24 hour as follows (n = 6). Standard 3-(4,5-dimethyl-2-thiazolyl)-2,5-diphenyl-2-H-tetrazolium bromide dimethyl sulfoxide (MTT) detections were conducted to check cells' proliferation, which mainly included the following procedures. First, 20 μL of 0.5% MTT (in PBS) (Aladdin, Shanghai, China) was added to each well. After 4-hour incubation in 37°C, the suspension medium was discarded. Then, 150 μL of DMSO (Aladdin, Shanghai, China) was added to each well. Finally, the absorbance of each well was measured using light of wavelength of 490 nm. Significant differences were examined using a *t*-test from SPSS 16.0 software. Differences were considered significant when $P < .05$.

Prussian Blue Staining

Cells were iron-loaded by growing them in supplemented medium that contained 2 mM ferric citrate ammonium (FAC) (Macklin, Shanghai, China) for 48 hours. Then, the cells were washed using PBS 3 times and were fixed in 4% paraformaldehyde (Macklin, Shanghai, China) for 15 minutes. Cells were washed using deionized water several times. Iron staining was performed using a Prussian blue staining assay kit (Solarbio, Shanghai, China) following standard procedures. Cells were stained for 30 minutes by potassium ferrocyanide in hydrochloric acid and then washed with deionized water several times and counterstained with Fast Red for 10 minutes. Digital pictures were taken using a Leica fluorescent microscope (DM4000B, Leica, Solms, Germany) under bright field conditions.

Iron Measurements by Inductively Coupled Plasma Mass Spectroscopy

Cellular iron content was detected by inductively coupled plasma mass spectroscopy (ICP-MS) (i CAP Q, Thermo Fisher Scientific, Shanghai, China). First, a cell pellet was dissolved in 3 mL HNO_3/H_2O_2 (4:1) solution. Then, the clear sample solution was tested by ICP-MS following standard procedures.

MRI Experiments

For phantom preparation, cells (6×10^6/group) were uniformly suspended in 0.1 cc of 1% agarose in the middle of long glass tubes. Except for the cell layer, both the upper and lower regions of the tubes were filled with 1% agarose gel. Three tubes were prepared in total; the first tube was filled with glioma cells with ferritin–EGFP expression (labeled as "+"), the second tube was filled with glioma cells with no ferritin–EGFP expression (labeled as "−"), and the last one was filled with pure 1% agarose (labeled as "0"). Note that all cells were incubated with 2 mM FAC for 48 hours. The 3 tubes were evenly inserted into 2% agarose in a disk-like 7 × 10-cm (height × diameter) container. Similarly, different concentrations of FAC tubes were prepared in 1% agarose in the long glass tubes. A multiecho, gradient echo technique was applied to estimate R2* (1/T2*), as iron content can be estimated from the change in R2* ($\Delta R2^* = R2'$) between the gel with iron and that without iron. Data were collected on a 3 T scanner (MAGNETOM Trio, Siemens Healthcare, Erlangen, Germany) equipped with a standard 12-channel

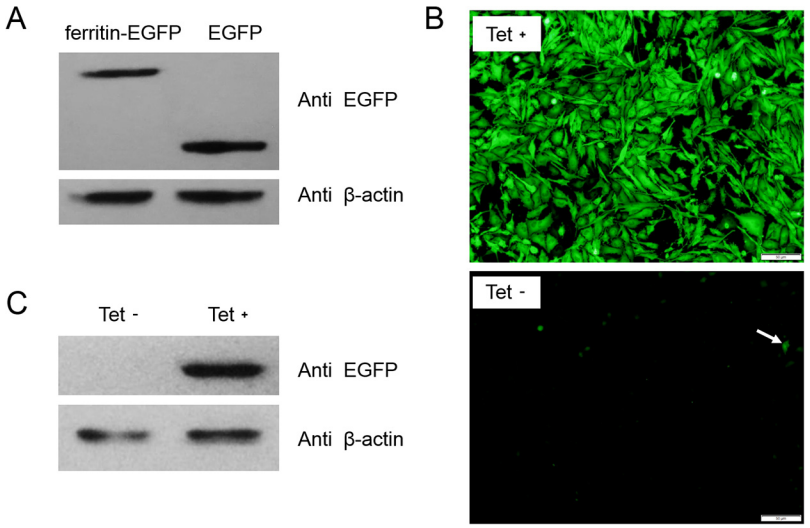

Figure 2. Ferritin–EGFP expressed in cells. Western blot detection of ferritin–EGFP. Left—ferritin–EGFP: HeLa cells' lysate transfected with pCEP4-ferritin–EGFP plasmids. Right—EGFP: HeLa cells' lysate transfected with pcDNA3.1-3′-EGFP plasmids (A). Fluorescence detection of tetracycline-inducible U251–TetR–ferritin–EGFP monoclonal cell strain (B). Upper—Tet+ group: ferritin–EGFP expression in U251–TetR–ferritin–EGFP monoclonal cells was started by adding tetracycline (2 μg/mL, 48 hours) into the cell culture medium. Lower—Tet− group: control groups, U251–TetR–ferritin–EGFP monoclonal cells cultured without any tetracycline. Scale = 50 μm. Western blot detection of U251–TetR–ferritin–EGFP monoclonal cell strain. Left—Tet− group: U251–TetR–ferritin–EGFP monoclonal cells lysate that was cultured without any tetracycline. Right—Tet+ group: U251–TetR–ferritin–EGFP monoclonal cells lysate, in which the ferritin–EGFP expression was started by adding tetracycline (2 μg/mL, 48 hours) into the cell culture medium (C). Note: Presence of anti-EGFP means the protein was detected by anti-EGFP antibodies, and presence of anti-β-actin means the protein was detected by anti-β-actin antibodies.

head coil. The imaging parameters for the 7 multiecho, gradient echo sequences were as follows: repetition time = 80 milliseconds, echo time = 10–70 milliseconds in increments of 10 milliseconds, flip angle = 25°, resolution = 0.27 × 0.27 × 1 mm, bandwidth = 120 Hertz/pixel, and sections = 80. R2* values were measured above, below, and in the region of iron content in the tubes containing cells using a rectangular region of 5228 pixels after zooming by a factor of 8 (roughly 82 pixels in the original unzoomed images).

RESULTS

Expression of Ferritin–EGFP in HeLa Cells and Glioma U251 Cells

The ferritin–EGFP produced here was a fusion protein and was composed of an EGFP (~27 kD), a ferritin heavy chain (~21 kD), and a polypeptide linker (~1.3 kD). Thus, its molecular weight was expected to be ~49 kD. Our Western blot result (Figure 2A) showed that ferritin–EGFP was successfully detected by anti-EGFP antibodies and showed a molecular weight much larger than that of EGFP, approaching 50 kD (protein marker was not shown). This proved that ferritin–EGFP was successfully expressed in cancer cells. Fluorescence detection showed that cells that expressed ferritin–EGFP emitted bright green fluorescence (Figure 2B), which indicated that the EGFP functioned well and was not impaired when linked with heavy-chain ferritin. Both of the above results show that ferritin–EGFP was successfully expressed in both HeLa cells and glioma U251 cells.

Establishment of a Tetracycline-Inducible U251–TetR–Ferritin–EGFP Monoclonal Cell Strain

A tetracycline-inducible U251–TetR–ferritin–EGFP monoclonal cell strain was successfully built through plasmid transfection and antibiotics screening. The tetracycline regulation system worked through the following mechanism: U251–TetR–ferritin–EGFP monoclonal cell strains could stably express both TetR and ferritin–EGFP. TetR bonded with tetracycline operator sequences ($TetO_2$) and thus suppressed the expression of the downstream gene (ferritin–EGFP gene in this case). But when tetracycline was present, TetR bonded with tetracycline and was structurally changed and detached from $TetO_2$, because of which, ferritin–EGFP suppression was relieved. When tetracycline was added (2 μg/mL, 48 hours), the ferritin–EGFP expression showed obvious protein expression as shown by both bright green fluorescence (Figure 2B, Tet+) and Western blot detection (Figure 2C, Tet+). When tetracycline was absent in the cell culture medium, the ferritin–EGFP expression was suppressed (Figure 2, B and C, Tet−). Usually, some low-level basal protein expression existed in tetracycline regulation systems; however, it could not be detected by Western blotting (Figure 2C, Tet−). Nevertheless, this low-level basal protein expression was successfully detected by fluorescence (Figure 2B, Tet−) and showed a weak, sparse green fluorescence signal (as indicated by the white arrow), which indicated that fluorescence detection was more sensitive than Western blotting. These interesting results

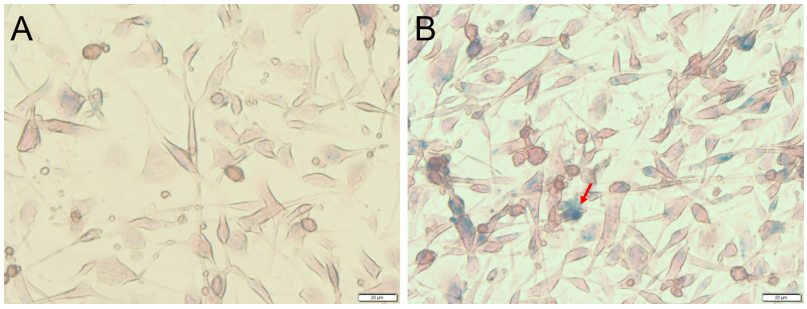

Figure 3. Prussian blue staining. Control group: U251cells that did not express ferritin–EGFP (A). Experimental group: U251 cells that express ferritin–EGFP (B). All cells were cultured in supplemented medium that contained 2 mM of ferric citrate ammonium (FAC) for 48 hours. Scale = 20 μm. Note: The blue particles indicated by the red arrow imply iron detected by Prussian blue staining.

revealed the high fluorescent sensitivity of ferritin–EGFP. In other words, we successfully established tetracycline-inducible U251–TetR–ferritin–EGFP monoclonal cell strain, and this cell strain worked stably even after 15 passages.

Cellular Iron Intake Observed by Prussian Blue Staining

In our experiments, both control group cells (that did not express any ferritin–EGFP) and experimental group cells (that stably expressed high levels of ferritin–EGFP) were iron-loaded with 2 mM FAC for 48 hours. Prussian blue staining (Figure 3) detected limited iron intake in the control group cells but detected obvious iron intake (blue particles shown by the red arrow) in the experimental group. Without FAC supplements, neither showed Prussian blue staining (data not shown). Because a small amount of native ferritin (compared with the large quantity of transgenic ferritin–EGFP) also existed in the cells (13), it was not surprising to observe some low-level iron intake in the control group with iron loading. However, the much higher level of iron intake in the experimental group indicated that the expression of ferritin–EGFP worked well as an iron-storage protein.

Effects of Ferritin–EGFP Overexpression on Cell Proliferation

Both control group cells (Tet−, without ferritin–EGFP expression) and experimental group cells (Tet+, with ferritin–EGFP expression) were evaluated every 24 hours to examine whether the ferritin–EGFP overexpression affects cell proliferation (Figure 4). The cell growth was monitored for 96 hours. A longer growth time may lead to an overgrowth of cells, causing large uncertainties in MTT detection. Significant differences were considered when $P < .05$. There were no significant differences between the 2 groups of cells when ferritin–EGFP expressed for 24, 48, 72 and 96 hours. Because the ferritin–EGFP expression was started by adding tetracycline (2 μg/mL for 48 hours) in the culture medium, the effects of tetracycline on cell proliferation were also examined through MTT detection. Results showed that tetracycline had no effect on cell growth, as no significant differences were observed between the experimental and control groups (Figure 5).

Cellular Iron Measurements by ICP-MS

The ICP-MS measurements (Figure 6) showed that the addition of iron (FAC) into the culture medium significantly increased cellular iron intake. Without iron supplement, limited iron was detected (about 0.11 pg/cell), whether or not the cells had ferritin–EGFP expression. However, with iron supplement, high levels of cellular iron were observed, particularly, measurements showed 5.1 pg/cell for the "Ferritin+" group and 3.9 pg/cell for the "Ferritin−" group. That is to say, ferritin expression promoted cellular iron intake by 31% compared with the control group (this was consistent with the Prussian blue results). However, the Prussian blue results showed less iron than the control

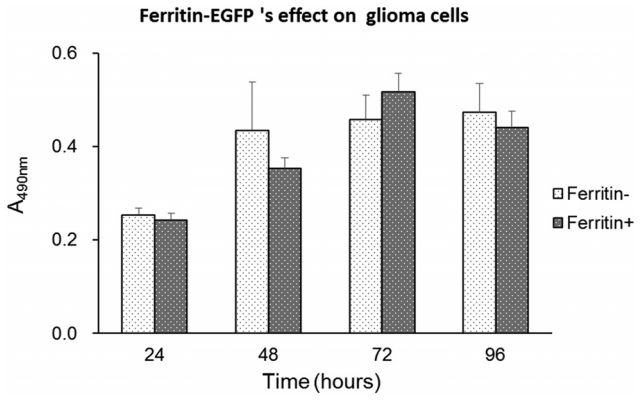

Figure 4. Effects of ferritin–EGFP expression on cell proliferation. Ferritin− was the control group; there was no tetracycline in the culture medium, so the ferritin–EGFP expression was suppressed. Ferritin+ was the experimental group, and there was tetracycline in the culture medium, so, it expressed high levels of ferritin–EGFP. Cells' proliferation was detected by 3-(4,5-dimethyl-2-thiazolyl)-2,5-diphenyl-2-H-tetrazolium bromide dimethyl sulfoxide (MTT) every 24 hours. Results are represented as mean ± SD (n = 6).

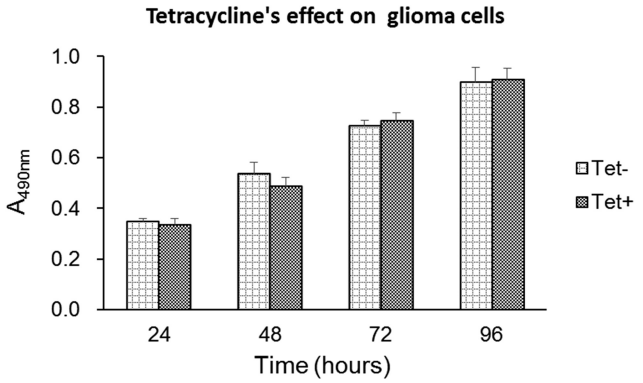

Figure 5. The effect of tetracycline on glioma cells. Normal glioma cells were used for this test. Tet− was the control group; there was no tetracycline in the culture medium. Tet+ was the experimental group; there was tetracycline in the culture medium. Cells' proliferation was detected by MTT every 24 hours. Results are represented as mean ± SD (n = 6).

group as shown by ICP-MS. This apparent difference could be caused by the detection sensitivities of the 2 methods. ICP-MS is capable of detecting lower levels of iron because it is much more sensitive than Prussian blue staining.

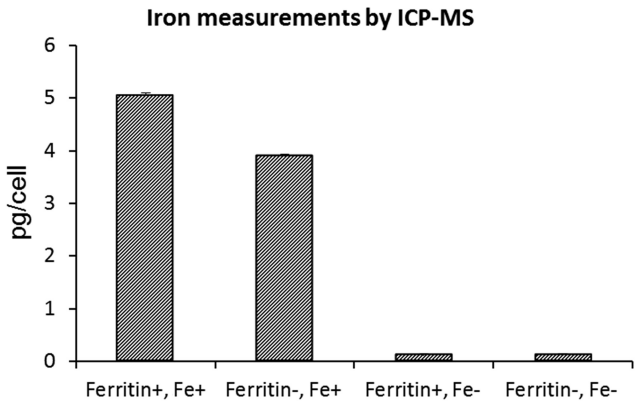

Figure 6. Cellular iron measurements by inductively coupled plasma mass spectroscopy (ICP-MS). "Ferritin+, Fe+": cells that express ferritin–EGFP and are supplemented with iron (FAC) during the culture process. "Ferritin−, Fe+": cells that do not express ferritin–EGFP but are supplemented with iron (FAC). "Ferritin+, Fe−": cells that express ferritin–EGFP but are not supplemented with iron (FAC). "Ferritin−, Fe−": cells that do not express ferritin–EGFP and are not supplemented with iron (FAC). Error bars are too small to be clearly seen.

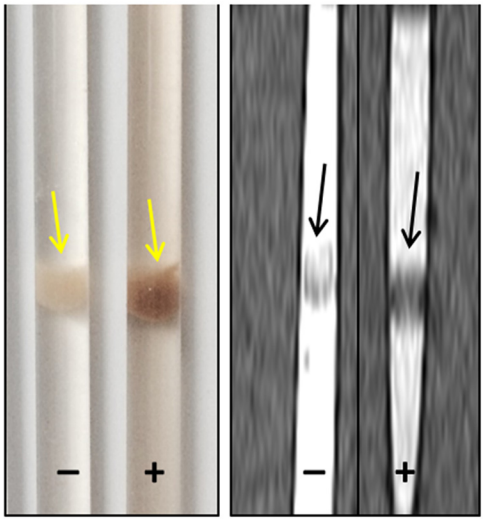

Figure 7. Left: photo of the tubes with no iron and with the iron-loaded cells. The brown layer has cell samples doped in it. Below and above the cells, the water was doped with 1% gel. Right: zoomed sagittal image of the tube showing signal reduction in the region of the iron-loaded cells. "−" means cells that do not express ferritin–EGFP and "+" means cells that express ferritin–EGFP. Both groups of cells were supplemented with iron during the culture process.

R2* Measurements and Estimation of Iron Content

Echo times of 10, 20, 30, and 40 milliseconds were used, as these provided the best image quality. R2* values were measured for 2 sections of cells in each tube (for visualization of the iron cell layers in the tubes themselves and the 40-millisecond image, see Figure 7). In each tube, 2 sections were evaluated. For the "Ferritin+" group, results for R2* were 35.3 ± 0.8/s in the iron-containing cell regions and 13.4 ± 0.2/s in the regions above and below the cells, yielding an R2′ of 21.9 ± 0.8/s. For the "Ferritin−" group, R2* was 27.5 ± 0.4/s in the iron-containing cell regions and 14.8 ± 0.1/s in the regions above and below the cells, yielding an R2′ of 12.7 ± 0.4/s. (All errors quoted are standard error of the mean over the ROI used.) Using the relationship $R2' = 2.2 + 50 \times [Fe]$ (mg Fe/g wet tissue) (22), giving 0.39 mg Fe/g wet tissue (6×10^6 cells) for the "Ferritin+" group and 0.21 mg Fe/g wet tissue for the "Ferritin−" group. These values predict ~6.5 ± 0.1 pg Fe/cell and 3.5 ± 0.02 pg Fe/cell for "Ferritin+" and "Ferritin−" groups, respectively.

DISCUSSION

This study aimed to establish an endogenous dual reporter for both fluorescence imaging and MRI by building a novel hybrid protein ferritin–EGFP. Fluorescence detection proved that ferritin–EGFP functioned well as a fluorescence reporter by emitting bright green fluorescence. The ferritin–EGFP expression led to a higher cellular iron content as shown by the results of Prussian blue staining, ICP-MS, and MRI measurements, all of

which indicated that ferritin–EGPF expression was effective as an MRI reporter.

Before this study, several dual reporters were successfully established, in which ferritin and fluorescent proteins were separately expressed, such as myc-ferritin and green fluorescent protein (13), ferritin and red fluorescent protein (23), and ferritin and EGFP (15). Nevertheless, fluorescent protein-fused ferritin was more favorable, as it was distinguishable from native ferritin inside cells. Ono et al. (24) found lower DsRed fluorescence in a DsRed–ferritin fusion protein, and they speculated that DsRed's structure or stability may be affected. In our study, a special 18-amino-acid-long polypeptide was added between ferritin and EGFP to avoid potential interferences between them. This polypeptide was expected to improve the performance of the EGFP reporter gene. When Kim et al. (21) studied the application of fluorescent ferritin nanoparticles to the aptamer sensor, they found that when EGFP was linked to the C terminal of heavy-chain ferritin by a flexible glycine-rich peptide, the emission intensity and stability of EGFP were both greatly improved because of the aggregation nature of the heavy-chain ferritin. Despite the fact that our EGFP was linked to a modified polypeptide, it still showed high fluorescent sensitivity, and its expression was successfully regulated by tetracycline.

The effects of ferritin overexpression have been controversial. Some studies found that ferritin may be an effective therapy for prevention and treatment of Parkinson disease by reducing reactive iron (25). Further, Ziv et al. (11) reported the follow-up of a transgenic mice that overexpressed H-ferritin in liver hepatocytes for 2 years, and found that ferritin overexpression was safe for the mice. However, there was also evidence showing damage caused by ferritin overexpression, such as cell growth inhibition (18) or progressive age-related neurodegeneration (26, 27). These findings may be caused by various ferritin expression levels. Therefore, we created a tetracycline-regulated ferritin–EGFP expression system to avoid potential harm and investigate the effects of ferritin at different expression levels.

Literature (14, 16) reported that ferritin overexpression is supposed to increase net iron uptake by improved transferrin receptor or intracellular iron redistribution even without iron supplements. However, as shown in our study, no obvious iron intake was observed (neither by Prussian blue staining nor by ICP-MS measurements) if there was no iron supplement in the culture medium. Instead, FAC supplement seems to be effective in increasing cellular iron intake. Ferritin expression enhanced this effect.

Although the estimates of iron content measured by MRI and ICP-MS are not in perfect agreement, they are only slightly different, and the relative values of each are similar. For the MR R2* estimates, as the 2 sections had equal volumes, a simple average of the values in the 2 sections was taken. The thickness of the cell layers and resolution of only 1-mm-thick sections made it difficult to incorporate partial volume effects, so we considered just the central 2 sections with clear signal changes. The iron in the "Ferritin−" group appears to have settled, giving a different R2* values for each layer, but the average R2* still represents the correct concentration of iron.

One can estimate iron loading and effective susceptibility from these measurements. Using 6 pg Fe/cell for 6 million cells gives 6.4×10^{10} atoms/cell. If there are 100 million ferritin proteins/cell; this predicts 640 iron atoms/ferritin. This lies in the loading range of 0–4500 iron atoms/ferritin known in the literature (10). One can also estimate the susceptibility in every cell using the following formula: $R2' = k\lambda\gamma\Delta\chi B_o$, where $k = 0.4$ for point dipoles, and here, $B_o = 3T$. Iron in the ferritin may take the form of 5 $Fe_2O_3{\cdot}9H_2O$, Fe_3O_4, or Fe_2O_3 (10). Using Fe_3O_4, the fact that the iron sits in 0.1 cc and the density of iron is 5.18 g/cc, the volume fraction of iron is estimated to be $\lambda = 6.95 \times 10^{-6}$. This yields a $\Delta\chi$ of $\sim 9.9 \times 10^4$ ppm or a $\Delta\chi$/cell of 1.65×10^{-4} ppm. This value is close to the nanoparticles' susceptibility (7.5×10^4 ppm at 3 T) used by Shen et al. (28). At 3 T, the noise in measuring $\Delta\chi$ using quantitative susceptibility mapping (29) with a 3-dimensional sequence covering the whole brain is about 20 ppb for a 1-mm^3 voxel size depending on the imaging parameters and imaging time. This suggests that it is possible to measure the presence of ~100 cells with a signal-to-noise ratio of ~8:1.

In summary, we successfully established a tetracycline-inducible ferritin–EGFP chimera. Our results confirm the potential to use this chimera as an endogenous dual reporter for both fluorescence imaging and MRI for cellular levels of ferritin–EGFP.

ACKNOWLEDGMENTS

We acknowledge Dr. Zhen Cao (Shanghai Key Laboratory of Magnetic Resonance, East China Normal University, Shanghai, China) for generously providing pcDNA4/TO-neo+ vector, Yu Wang for helping with MRI data processing, Dr. Lan Fang (Institute of Biomedical Sciences, East China Normal University, Shanghai, China) for HeLa Cells, and Dr. Yunfei Chen (Institute of Biomedical Sciences, East China Normal University, Shanghai, China) for pcDNA3.1-3′-EGFP vector. We thank Dr. Wei Zhang and Changguo Gong (School of Life Sciences, East China Normal University, Shanghai, China) for the use of their fluorescent microscope and their technical assistance in performing the fluorescence imaging. We also thank Paul Kokeny and Kia Ghasaban for useful discussions and help with references.

Disclosures: No disclosures to report.

Conflict of Interest: None reported.

REFERENCES

1. Huse JT, Holland EC. Targeting brain cancer: advances in the molecular pathology of malignant glioma and medulloblastoma. Nat Rev Cancer. 2010;10(5):319–331.
2. Arena F, Singh JB, Gianolio E, Stefania R, Aime S. β-Gal gene expression MRI reporter in melanoma tumor cells. Design, synthesis, and in vitro and in vivo testing of a Gd(III) containing probe forming a high relaxivity, melanin-like structure upon β-Gal enzymatic activation. Bioconjug Chem. 2011;22(12):2625–2635.
3. Bulte JW, Kraitchman DL. Iron oxide MR contrast agents for molecular and cellular imaging. NMR Biomed. 2004;17(7):484–499.
4. Gutova M, Frank JA, D'Apuzzo M, Khankaldyyan V, Gilchrist MM, Annala AJ, Metz MZ, Abramyants Y, Herrmann KA, Ghoda LY, Najbauer J, Brown CE, Blanchard MS, Lesniak MS, Kim SU, Barish ME, Aboody KS, Moats RA. Magnetic resonance imaging tracking of ferumoxytol-labeled human neural stem cells: studies leading to clinical use. Stem Cells Transl Med. 2013;2(10):766–775.
5. Matuszewski L, Persigehl T, Wall A, Schwindt W, Tombach B, Fobker M, Poremba C, Ebert W, Heindel W, Bremer C. Cell tagging with clinically approved iron oxides: feasibility and effect of lipofection, particle size, and surface coating on labeling efficiency. Radiology. 2005;235(1):155–161.

6. Bowen CV, Zhang X, Saab G, Gareau PJ, Rutt BK. Application of the static dephasing regime theory to superparamagnetic iron-oxide loaded cells. Magn Reson Med. 2002;48(1):52–61.
7. Vande Velde G, Himmelreich U, Neeman M. Reporter gene approaches for mapping cell fate decisions by MRI: promises and pitfalls. Contrast Media Mol Imaging. 2013;8(6):424–431.
8. Vandsburger MH, Radoul M, Cohen B, Neeman M. MRI reporter genes: applications for imaging of cell survival, proliferation, migration and differentiation. NMR Biomed. 2013;26(7):872–884.
9. Arosio P, Levi S. Ferritin, iron homeostasis, and oxidative damage. Free Radic Biol Med. 2002;33(4):457–463.
10. Aisen P, Enns C, Wessling-Resnick M. Chemistry and biology of eukaryotic iron metabolism. Int J Biochem Cell Biol. 2001;33(10):940–959.
11. Ziv K, Meir G, Harmelin A, Shimoni E, Klein E, Neeman M. Ferritin as a reporter gene for MRI: chronic liver over expression of H-ferritin during dietary iron supplementation and aging. NMR Biomed. 2010;23(5):523–531.
12. Liu J, Cheng EC, Long RC, Yang SH, Wang L, Cheng PH, Yang J, Wu D, Mao H, Chan AW. Noninvasive monitoring of embryonic stem cells in vivo with MRI transgene reporter. Tissue Eng Part C Methods. 2009;15(4):739–747.
13. Kim HS, Cho HR, Choi SH, Woo JS, Moon WK. In vivo imaging of tumor transduced with bimodal lentiviral vector encoding human ferritin and green fluorescent protein on a 1.5T clinical magnetic resonance scanner. Cancer Res. 2010; 70(18):7315–7324.
14. Cohen B, Dafni H, Meir G, Harmelin A, Neeman M. Ferritin as an endogenous MRI reporter for noninvasive imaging of gene expression in C6 glioma tumors. Neoplasia. 2005;7(2):109–117.
15. Wilkinson J 4th, Di XM, Schonig K, Buss JL, Kock ND, Cline JM, Saunders TL, Bujard H, Torti SV, Torti FM. Tissue-specific expression of ferritin H regulates cellular iron homoeostasis in vivo. Biochem J. 2006;395(3):501–507.
16. Cohen B, Ziv K, Plaks V, Israely T, Kalchenko V, Harmelin A, Benjamin LE, Neeman M. MRI detection of transcriptional regulation of gene expression in transgenic mice. Nat Med. 2007;13(4):498–503.
17. Friedman A, Arosio P, Finazzi D, Koziorowski D, Galazka-Friedman J. Ferritin as an important player in neurodegeneration. Parkinsonism Relat Disord. 2011; 17(6):423–430.
18. Guo JH, Juan SH, Aust SD. Suppression of cell growth by heavy chain ferritin. Biochem Biophys Res Commun. 1998;242(1):39–45.
19. Festa M, Ricciardelli G, Mele G, Pietropaolo C, Ruffo A, Colonna A. Overexpression of H ferritin and up-regulation of iron regulatory protein genes during differentiation of 3T3-L1 pre-adipocytes. J Biol Chem. 2000;275(47):36708–36712.
20. Pham CG, Bubici C, Zazzeroni F, Papa S, Jones J, Alvarez K, Jayawardena S, De Smaele E, Cong R, Beaumont C, Torti FM, Torti SV, Franzoso G. Ferritin heavy chain upregulation by NF-kappaB inhibits TNFalpha-induced apoptosis by suppressing reactive oxygen species. Cell. 2004;119(4):529–542.
21. Kim S-E, Ahn K-Y, Park J-S, Kim KR, Lee KE, Han S-S, Lee J. Fluorescent ferritin nanoparticles and application to the aptamer sensor. Anal Chem. 2011;83(15): 5834–5843.
22. Gelman N, Gorell JM, Barker PB, Savage RM, Spickler EM, Windham JP, Knight RA. MR imaging of human brain at 3.0 T: preliminary report on transverse relaxation rates and relation to estimated iron content. Radiology. 1999;210(3):759–767.
23. Aung W, Hasegawa S, Koshikawa-Yano M, Obata T, Ikehira H, Furukawa T, Aoki I, Saga T. Visualization of in vivo electroporation-mediated transgene expression in experimental tumors by optical and magnetic resonance imaging. Gene Ther. 2009;16(7):830–839.
24. Ono K, Fuma K, Tabata K, Sawada M. Ferritin reporter used for gene expression imaging by magnetic resonance. Biochem Bioph Res Commun. 2009;388(3): 589–594.
25. Kaur D, Yantiri F, Rajagopalan S, Kumar J, Mo JQ, Boonplueang R, Viswanath V, Jacobs R, Yang L, Beal MF, DiMonte D, Volitaskis I, Ellerby L, Cherny RA, Bush AI, Andersen JK. Genetic or pharmacological iron chelation prevents MPTP-induced neurotoxicity in vivo: a novel therapy for Parkinson's disease. Neuron. 2003;37(6):899–909.
26. Kaur D, Rajagopalan S, Chinta S, Kumar J, Di Monte D, Cherny RA, Andersen JK. Chronic ferritin expression within murine dopaminergic midbrain neurons results in a progressive age-related neurodegeneration. Brain Res. 2007;1140:188–194.
27. Kaur D, Peng J, Chinta SJ, Rajagopalan S, Di Monte DA, Cherny RA, Andersen JK. Increased murine neonatal iron intake results in Parkinson-like neurodegeneration with age. Neurobiol Aging. 2007;28(6):907–913.
28. Shen Y, Cheng YC, Lawes G, Neelavalli J, Sudakar C, Tackett R, Ramnath HP, Haacke EM. Quantifying magnetic nanoparticles in non-steady flow by MRI. MAGMA. 2008;21(5):345–356.
29. Haacke EM, Liu S, Buch S, Zheng W, Wu D, Ye Y. Quantitative susceptibility mapping: current status and future directions. Magn Reson Imaging. 2015;33(1):1–25.